

Antennal Lobe Processing Increases Separability of Odor Mixture Representations in the Honeybee

Nina Deisig,^{1,2} Martin Giurfa,^{1,2} and Jean Christophe Sandoz^{1,2}

¹Research Centre for Animal Cognition (UMR 5169), Université de Toulouse, UPS; and ²Research Centre for Animal Cognition (UMR 5169), Centre National de la Recherche Scientifique, Toulouse, France

Submitted 17 April 2009; accepted in final form 19 February 2010

Deisig N, Giurfa M, Sandoz JC. Antennal lobe processing increases separability of odor mixture representations in the honeybee. *J Neurophysiol* 103: 2185–2194, 2010. First published February 24, 2010; doi:10.1152/jn.00342.2009. Local networks within the primary olfactory centers reformat odor representations from olfactory receptor neurons to second-order neurons. By studying the rules underlying mixture representation at the input to the antennal lobe (AL), the primary olfactory center of the insect brain, we recently found that mixture representation follows a strict elemental rule in honeybees: the more a component activates the AL when presented alone, the more it is represented in a mixture. We now studied mixture representation at the output of the AL by imaging a population of second-order neurons, which convey AL processed odor information to higher brain centers. We systematically measured odor-evoked activity in 22 identified glomeruli in response to four single odorants and all their possible binary, ternary and quaternary mixtures. By comparing input and output responses, we determined how the AL network reformats mixture representation and what advantage this confers for odor discrimination. We show that increased inhibition within the AL leads to more synthetic, less elemental, mixture representation at the output level than that at the input level. As a result, mixture representations become more separable in the olfactory space, thus allowing better differentiation among floral blends in nature.

INTRODUCTION

The architecture of central primary olfactory centers is similar in vertebrates and insects. Both the vertebrate olfactory bulb (OB) and the insect antennal lobe (AL) consist of glomeruli, which receive input from olfactory receptor neurons (ORNs) expressing the same receptor type (Mombaerts et al. 1996; Vosshall et al. 2000). Glomeruli are interconnected by different sets of local neurons, which are mostly inhibitory and reformat odor representations in the form of a stimulus-dependent, spatiotemporal redistribution of activity across the AL/OB. The processed signals are further conveyed to higher-order centers by output neurons, the projection neurons (PNs) in insects, and the mitral/tufted cells in vertebrates (Fig. 1A; Bhandawat et al. 2007; Laurent 2002; Root et al. 2007; Sachse and Galizia 2002; Wachowiak and Shipley 2006).

In *Drosophila*, studies on odor coding using single odor molecules have shown nonlinear signal transformation in the AL (Bhandawat et al. 2007; Wilson et al. 2004), which seems to increase separability among odor representations. However, whether such a principle applies to odor mixtures remains unknown because most studies on the neural reformatting of odor representations have essentially used single odorants

(Bhandawat et al. 2007; Ng et al. 2002; Wang et al. 2003; Wilson et al. 2004). Because natural odors are complex blends including many different components, studying how the neural code for olfactory mixtures is reshaped by AL processing is imperative to understand odor processing in a natural framework. At the OB/AL input level, mixture representation follows essentially elemental rules because it can be predicted from the responses to the components (Carlsson et al. 2007; Deisig et al. 2006; Silbering and Galizia 2007; Tabor et al. 2004). By contrast, at the AL output level, strong interactions between component signals within the AL networks were found in the zebrafish (Tabor et al. 2004) and *Drosophila* (Silbering and Galizia 2007), assigning unique properties to each mixture's representation and making it different from the sum of its components. It is still unclear whether such nonlinear interactions are a by-product of local processing or whether they provide an actual benefit for mixture discrimination.

Using *in vivo* optical imaging in honeybees, we previously recorded the calcium responses to four single odors and all their possible mixture combinations in a set of well-identified olfactory glomeruli (Deisig et al. 2006). By bath-applying the calcium-sensitive dye Calcium Green-2 AM on the brain, we recorded a compound signal dominated by sensory input (see DISCUSSION). In the present study, to unravel the transformation of mixture representation within the AL network, we backfilled a population of PNs with the calcium-sensitive dye fura-2 dextran and recorded the calcium responses of the same glomeruli to the same four single odors and all their possible mixture combinations. Thus input and output mixture representations could be compared. We show that PN mixture representation is the result of subtle reformatting within the AL, which makes similarity relationships between mixture and components less predictable based on component information, i.e., less elemental. Furthermore, we show for the first time that such nonelemental reformatting increases separability among odor mixtures, thus facilitating olfactory mixture discrimination.

METHODS

Preparation and staining

Worker honey bees (*Apis mellifera*) were caught at the entrance of outdoor hives, cooled on ice, and mounted in Plexiglas chambers. The antennae were oriented to the front and their base was fixed with two-component silicon (KwikSil; World Precision Instruments, Sarasota, FL), providing a seal between the flagella (remaining in the air for odor stimulation) and the brain (under Ringer solution for optical imaging). The head capsule was then opened and all glands, membranes, and trachea were removed to reveal the two antennal lobes

Address for reprint requests and other correspondence: J. C. Sandoz, Evolution, Genome and Speciation, CNRS (UPR 9034), Avenue de la Terrasse, 91198 Gif-sur-Yvette, France (E-mail: sandoz@legs.cnrs-gif.fr).

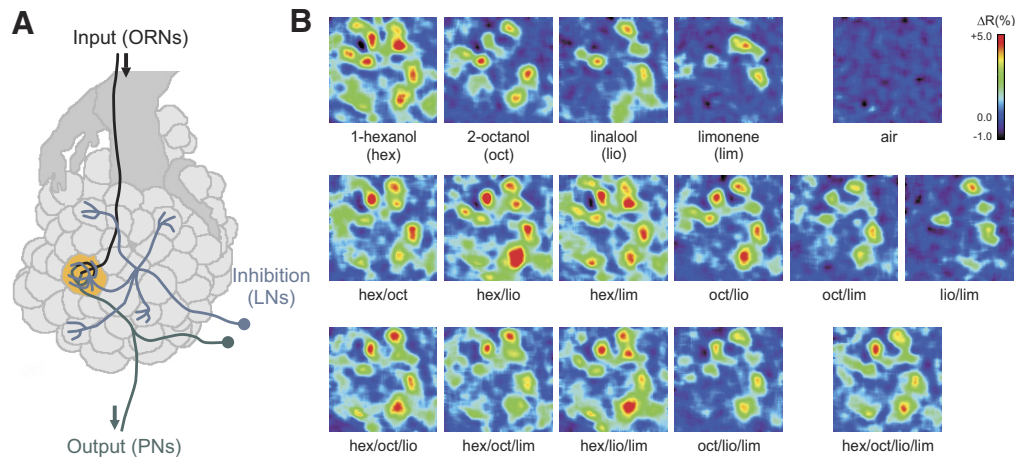


FIG. 1. Schematic view of the antennal lobe (AL) and odor-induced calcium activity from a population of second-order neurons (projection neurons [PNs]) in the honeybee AL. *A*: schematic view of the AL showing its glomerular structure and including the incoming (olfactory receptor neurons [ORNs], black) and outgoing (PNs, green) information pathways, as well as the local network of inhibitory interneurons (LNs, blue). *B*: the activity patterns present the amplitude of the calcium response obtained in one bee to 4 individual odorants and all the possible binary, ternary, and quaternary mixtures. The activity patterns are represented according to a common intensity scale (F_{340}/F_{380} ratio, *top right*). In all cases (except the air control), combinations of glomeruli were activated to the individual odorants and their mixtures.

(ALs). The brain was regularly washed with Ringer (in mM: NaCl, 130; KCl, 6; CaCl_2 , 5, MgCl_2 , 4; sucrose, 160; glucose, 25; HEPES, 10; pH 6.7, 500 mOsmol; all chemicals were from Sigma-Aldrich, Lyon, France) and before staining, illumination was reduced and switched to red light. In this work we specifically stained according to the protocol proposed by Sachse and Galizia (2002) projection neurons conveying odor information through the lateral antennocerebral tract (l-ACT) from the AL to the mushroom bodies and the lateral horn using fura-2 dextran (10,000 MW, in 2% BSA; Molecular Probes). After staining, the brain was thoroughly washed with saline and the bee was left in a dark place for 3 h.

Optical recordings of odor-evoked activity

In vivo calcium imaging recordings were done using an epifluorescent microscope (Olympus BX-51WI) with a $\times 20$ (NA 0.5) water immersion objective (Olympus UMPlanFL) and imaging system (TILL Photonics, Gräfeling, Germany). Images were taken using a 640×480 pixel 12-bit monochrome charge-coupled device camera (T.I.L.L. Imago) cooled to -12°C . The preparation was alternately excited with 340 and 380 nm monochromatic light (T.I.L.L. Polychrom IV). Each recording consisted of 100 double frames, at a rate of 5 double frames/s. We used 4×4 binning on chip (pixel size corresponds to $\sim 2 \times 2 \mu\text{m}$). Integration time was 16–32 and 4–8 ms, respectively, for 340 and 380 nm excitation. Odor stimuli were applied just before the beginning of the 15th double frame until the 20th double frame (i.e., odor lasted 1 s) using a computer-driven odor supplying device as in Deisig et al. (2006). The primary odors were 1-hexanol, 2-octanol, \pm linalool, and limonene (Sigma-Aldrich), each applied pure at a dose of $4 \mu\text{l}$ on 1 cm^2 filter paper strips, which were separately inserted in individual 0.7 ml syringes and mounted in the odor-supplying device. In the case of mixture stimulation, the airflow was directed into the syringes containing the odor components, mixing them only during stimulation, so that single odors could not interact chemically but added up in the mixture. Each bee was subjected to up to three runs of 17 stimulations, each including the four primary odors (A, B, C, and D), their binary (AB, AC, AD, BC, BD, and CD), ternary (ABC, ACD, BCD, and ABD), and quaternary (ABCD) mixtures as well as air and 1-nonanol, included as controls (the latter for monitoring the quality of the recording). The order of odor presentations was randomized between bees. The interval between stimulations was 80 s. For analysis, only complete runs were kept and different runs were averaged before further analysis. In all, nine bees were used in the analyses.

Mapping of glomeruli

Visualization of the glomerular AL structure after functional optical imaging was obtained according to Sandoz (2006). The brain was soon treated with a protease and 4% neutral red in distilled water. Fluorescence photographs allowed visualization and identification of 22 glomeruli in all preparations, based on the standardized AL atlas (Galizia et al. 1999). From these, 21 were imaged in a previous study (Deisig et al. 2006) and were used for comparisons between processing levels. This population of imaged glomeruli has proved to account for olfactory behavioral performances of bees (Guerrieri et al. 2005).

Raw data processing

Analysis of calcium-imaging data was carried out using IDL 6.3 (Research Systems, Boulder, CO). Each recording to an odor stimulus corresponded to a four-dimensional array with the excitation wavelength (340 or 380 nm), two spatial dimensions (x, y pixels of the area of interest), and the temporal dimension (100 frames). Three steps were carried out to calculate the signals (Galizia and Vetter 2005). First, to correct for bleaching at each wavelength (340 and 380 nm), a logarithmic decline curve fitted to mean fluorescence decay was subtracted from the whole image. The 5 s following odor onset were not included in the fitting process. Such a correction stabilizes the baseline of the recordings, without affecting odor-evoked responses. Second, we performed at each wavelength (340 and 380 nm) a scattered light correction, as done by Peele et al. (2006). Such a correction reattributes scattered light, avoiding that glomeruli with strong activity cause fictive activity in neighboring silent glomeruli. We then calculated $F'_n = F_n + 3[F_n - \text{sm}(F_n)]$, where F_n corresponds to frame number n and $\text{sm}(F_n)$ represents F_n after treatment with a boxcar filter (kernel size $50 \mu\text{m}$, i.e., 25 pixels). Third, for each pixel, we calculated the ratio R of the 340 and the 380 nm data. Then, $\Delta R_n = R_n - R_0$ was calculated, in which R_n is the ratio data at frame n and R_0 is the average of a few frames before the stimulus (frames 5–13). Thus ΔR is close to 0 shortly before the odor stimulus and shows throughout a recording the relative variations of the ratio. For quantitative analysis of the data, the time course of ΔR was calculated by averaging 49 pixels (7×7) at the center of each identified glomerulus and well within its borders. Then, amplitude of the odor-induced response of each glomerulus was calculated by subtracting the mean of 3 frames during the odor (frames 17–19) from the mean of 3 frames before the stimulus (frames 12–14). This time window corresponded

to the moment of maximal separation power between odor response and baseline (see Supplemental Fig. S6).¹ This value was then used in all computations. For the presentation of activity maps (Fig. 1), the amplitude of odor-induced responses within each pixel was calculated as before. The resulting image was then subjected to a boxcar filter of kernel size 9 pixels and presented in a false color code of increasing amplitude from dark blue to red.

Data analysis

The goal of the present study was to compare the rules underlying olfactory-mixture representation between the input (as measured from the compound signal using bath-application of Calcium Green-2 AM; Deisig et al. 2006) and the output (measured by specific staining of the projection neurons with fura-2 dextran; this study). We first used an analysis rationale similar to that in the initial study, analyzing the relationships between mixture- and component-induced signals, both at the level of individual glomeruli and considering the whole glomerular pattern accessible to us. We also provided a range of novel analyses comparing the linearity of mixture representation between input and output and the separation power between odor representations achieved at these two levels.

NUMBER OF ACTIVE GLOMERULI. We recorded dendritic calcium signals from I-ACT PNs in AL glomeruli. Previous experiments have shown that these glomerular calcium responses correlate closely with the action potential activity of these PNs (Galizia and Kimmerle 2004). Thus calcium signals from PN dendrites are a monitor for the activity of PNs at the output side of the glomerulus (Szyszka et al. 2005). We asked how the magnitude of PN activity changes with added mixture components. We thus measured the number of glomeruli in which the recorded dendritic PN signal was above noise level (see following text), later termed “active glomeruli” for easier reference. Noise was defined as 4SD of the signal within each glomerulus before the stimulus (frames 1–14). The proportion of excitatory and inhibitory signals was determined from signals respectively above +4SD or below –4SD. Since inhibitory responses were very few, analysis concentrated on excitatory responses. The number of activated glomeruli was compared among mixture types (single odor, binary, ternary, and quaternary mixtures) or among single odors, using repeated-measure ANOVAs whenever possible (equal observation numbers).

MIXTURE INTERACTIONS. For evaluation of possible mixture interactions at the level of single glomeruli, the response classification method was the same as that used in Deisig et al. (2006). For each glomerulus the response to a mixture and the response to the strongest component were compared. The strongest component was defined as the component of the mixture inducing the highest response in the considered glomerulus. The response to the mixture could be higher than (“synergy”), equal to (“hypoadditivity”), or lower than (“suppression”) the response to the strongest component. A minimum difference of 15% on normalized data (each bee’s maximum glomerular response being set to 100%) was used as the threshold for deciding whether responses to stimulus X and Y were different. This threshold was determined previously from the average SD of primary odor responses (Deisig et al. 2006) and has been kept here to allow direct comparison between input and output data sets.

SIMILARITY BETWEEN MIXTURE REPRESENTATIONS. Multivariate analyses were used to classify the different mixtures and components according to their proximity in a putative neural olfactory space constructed on the basis of PN responses (Fig. 3B). The neural representation of an odor can be regarded as a vector in a multidimensional space, in which each dimension is represented by a particular glomerulus. Evaluation of the relationships between the repre-

sentation of each mixture and the representations of its components was calculated using a Euclidean metric. The distance d between two odors i and j was calculated as

$$d_{ij} = \sqrt{\sum_{k=1}^p (X_{ik} - X_{jk})^2}$$

where p is the number of dimensions (i.e., glomeruli) and X_{ik} and X_{jk} are the responses in glomerulus k to odors i and j , respectively.

Since it is not possible to visualize vectors in an n -dimensional space, a principal component analysis (PCA) was used to project the data into a lower-dimensionality space formed of a subset of highest-variance components. In addition, a cluster analysis using Ward’s classification method was performed to group single odors and mixtures according to their respective distances in the PN olfactory space.

ELEMENTAL MODEL OF MIXTURE REPRESENTATION. Similarity between neural representations of mixtures and their components was quantified in terms of the Euclidean distance separating them in a putative olfactory space, in which each dimension represents activity of one of the recorded glomeruli. For each mixture’s component, its distance to the mixture was calculated, relative to the sum of the distances of all components to the mixture (Fig. 4 and Supplemental Fig. S4). This relative distance was calculated as

$$D_{i,mix} = \frac{d_{i,mix}}{\sum_{k=1}^p d_{k,mix}}$$

where i indicates a component, mix is the mixture, p is the number of components in the mixture, and $d_{k,mix}$ is the Euclidean distance between a component k and the mixture in the putative olfactory space (for a calculation example, see Fig. 7A in Deisig et al. 2006). Thus for binary, ternary, and quaternary mixtures, equidistance between a mixture and its components corresponds to relative distances $D_{i,mix}$ of 50, 33.3, and 25%, respectively. To provide a measure of relative distance that is independent of component number (p), the relative distance index was calculated as $D'_{i,mix} = p \times D_{i,mix}$. Thus in all cases, equidistance corresponded to a value of 1. For each mixture component, its divergence from equidistance was calculated as the absolute value of $D'_{i,mix} - 1$. To evaluate how much odor representation differed from equidistance at the two processing levels, these divergence values were compared between PNs and compound signal data sets using a paired t -test (Fig. 4B).

To test whether the representation of a mixture follows those of the components (elemental model), the relative Euclidean distances between mixture and each of its components were compared with the relative “weight” of the components in the mixture $W_{i,mix}$. Such weight is given by the magnitude of the response (number of activated glomeruli) to the component when presented alone, relative to the sum of response magnitudes of all components of the mixture. Thus the relative “weight” (W) of a component in a mixture was

$$W_{i,mix} = \frac{N_i}{\sum_{k=1}^p N_k}$$

where i indicates a component, mix is the mixture, p is the number of components in the mixture, and N_k is the number of active glomeruli when presenting odor k alone (for a calculation example, see Fig. 7B in Deisig et al. 2006). To provide a relative weight that is independent of the number of components, we calculated the relative weight index as $W'_{i,mix} = p \times W_{i,mix}$. Thus for all mixtures, components having an equal weight would yield $W'_{i,mix} = 1$. We then determined the

¹ The online version of this article contains supplemental data.

relationship between $D'_{i,mix}$ and $W'_{i,mix}$, which gives an overall evaluation of the quality of the model, independently of the number of mixture components. All linear correlations were tested for significance by calculating Pearson's r and using a t -test (Zar 1999; Fig. 4C). To compare the efficacy of the correlation obtained for AL input (compound signal) and output (PNs), we compared correlation coefficients using a homogeneity t -test.

SEPARABILITY OF ODOR STIMULI. Because PN and compound signals had different amplitudes, the Euclidean distances between the two data sets could not be directly compared. We thus used two different methods to compare separability at AL input and output levels. First, we calculated Euclidean distances on normalized data sets—i.e., by normalizing responses in all glomeruli to all odors according to the highest glomerular response observed in this data set (Fig. 5). Second, we used Pearson's correlation coefficient r as a measure of similarity between odor representations (Supplemental Fig. S5), which is independent of response amplitude (Peele et al. 2006; Sachse et al. 1999, 2002). Both methods gave the same results, thus underlining the robustness of our data.

RESULTS

Calcium signals from projection neurons

Using the calcium sensitive dye fura-2 dextran, we performed recordings from a population of uniglomerular projection neurons belonging to the lateral-antennal glomerular tract (L-ACT), which conveys olfactory information from the AL to higher-order centers such as the mushroom bodies and the

lateral horn. Bees were stimulated with four single odors and all their binary, ternary, and quaternary mixtures. All stimuli induced activity in a combination of glomeruli, whereas air stimulation had no effect (Fig. 1B, example for one bee). Signals were mostly excitatory (98.8%, phasic or phasic-tonic; e.g., Fig. 2A), showing an increase in calcium concentration on stimulation, which is in accordance with previous PN recordings in the honeybee (Peele et al. 2006; Szyszka et al. 2005).

Number of activated glomeruli

When considering the intensity of glomerular activation on single odorant and mixture stimulation, we found output response properties similar to those previously recorded at AL input (compound signal; Deisig et al. 2006). First, the four primary odorants yielded a significant heterogeneity in glomerular activation when PN responses were quantified [repeated-measures ANOVA, $F_{(3,24)} = 5.88$, $P < 0.004$; Supplemental Fig. S1A], as at the input (Deisig et al. 2006). In both data sets, the primary odors 1-hexanol and 2-octanol induced stronger activation (8.3 ± 1.7 and 7.9 ± 1.2 activated glomeruli, respectively; means \pm SE), whereas linalool and limonene induced weaker activation (5.4 ± 1.2 and 3.8 ± 0.7 activated glomeruli, respectively). Second, in both data sets, the number of activated glomeruli strongly saturated with an increasing number of components in the mixture. In the case of PNs, no significant difference was found between stimuli with an in-

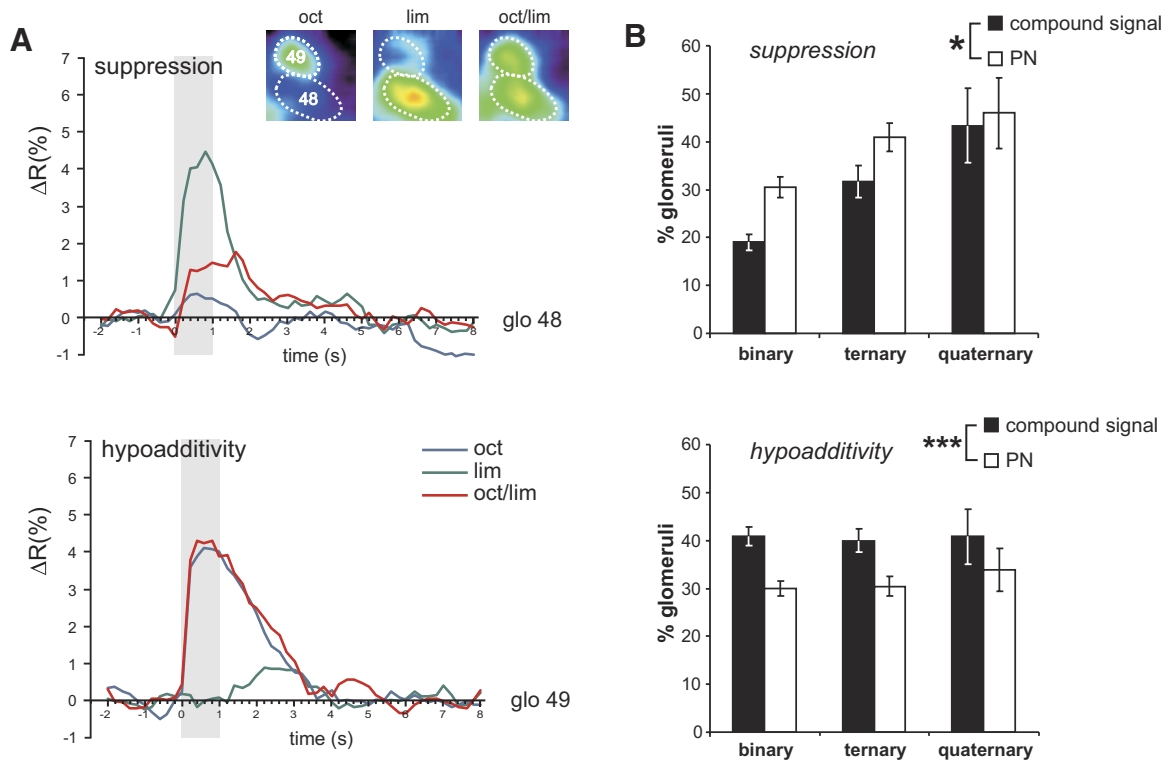


FIG. 2. Antennal lobe processing shows stronger influence of lateral inhibition. Repartition of glomerular responses in classes, depending on how the response to a mixture relates to the highest response (response to the “strongest component”). The different cases relate in psychophysical terms to phenomena of suppression (response to the mixture is below the response to the strongest component), hypoadditivity (response to the mixture is equal to that to the strongest component), or synergy (response to the mixture is higher than that to the strongest component). **A:** examples of calcium responses belonging to the suppression and hypoadditivity classes in 2 neighbor glomeruli, 48 and 49, corresponding to the presentations of 2-octanol, limonene, and their binary mixture. The graphs present the relative variations (in %) of the F_{340}/F_{380} ratio throughout a recording. The gray bar represents odor stimulation. **B:** comparison of the proportions of suppression and hypoadditivity cases (mean \pm SE %) between recordings at the input (compound signal, $n = 10$; Deisig et al. 2006) and at the output (PNs, $n = 9$, this study) of the AL (population \times component number ANOVA, $*P < 0.05$; $***P < 0.001$).

creasing number of components [Supplemental Fig. S1B: ANOVA, $F_{(3,131)} = 0.19$, NS]. Third, response magnitudes to the 15 odor stimuli were significantly correlated between AL input and output (Supplemental Fig. S2C, $r = 0.70$, $P < 0.01$, degrees of freedom [df] = 13). Fourth, for all odors and all glomeruli, the amplitudes of calcium responses were highly correlated between the two data sets (data not shown; $r = 0.59$, $P < 0.001$, df = 312). A significant correlation was found between PN and compound signal activity patterns in 12 of 15 cases ($r > 0.43$, $P < 0.05$, df = 19). This correlation was significantly higher for primary and binary olfactory stimulations ($r = 0.60 \pm 0.03$) than that for ternary and quaternary ones ($r = 0.47 \pm 0.04$; $t = 2.67$, $P = 0.02$, df = 13). These data show that AL local processing maintains similar quantitative relationships between the four single odorants or between mixtures with increasing numbers of components.

Mixture interactions at the glomerular level

Average PN activity maps were constructed for the nine bees tested (Supplemental Fig. S2). Although AL output activity patterns were qualitatively similar to AL input patterns, some glomeruli were exclusively activated in the compound signal data and others rather exclusively in the PN data. As at the input, a glomerulus exhibited PN activity on mixture stimulation when it was activated by at least one of its components. However, directly comparing the amplitudes of mixture and component responses revealed mixture responses that could not be easily predicted from the response to the components. PN responses were thus classified according to categories defined by Duchamp-Viret et al. (2003) (for details see Deisig et al. 2006). Most glomeruli showed suppression (lower response to the mixture than that to the most effective component; Fig. 2A, top) and hypoadditivity (equal responses to the mixture and to the most effective component; Fig. 2A, bottom), whereas cases of synergy (higher response to the mixture than that to the most effective component; not shown) were rare. We found that increasing the number of mixture components significantly increased suppression [Supplemental Fig. S3, ANOVA, $F_{(2,96)} = 5.77$, $P < 0.005$], whereas the number of hypoadditivity and of synergy cases did not change [respectively, $F_{(2,96)} = 0.40$, NS and $F_{(2,96)} = 0.21$, NS]. A substantial difference appeared between AL input and output at this level (Fig. 2B): PN signals showed significantly more suppression than that shown by compound signals [population \times component number ANOVA, population effect: $F_{(1,203)} = 6.11$, $P = 0.014$; component number effect: $F_{(2,203)} = 16.9$, $P < 0.001$], and logically less hypoadditivity [population effect: $F_{(1,203)} = 13.6$, $P < 0.001$; component number effect: $F_{(2,203)} = 0.19$, NS]. This indicates that local networks in the AL produce increased suppression of mixture activity at AL output relative to its input.

Similarity between mixture and single odor representations

We evaluated similarity relationships between odor representations on the basis of Euclidean distances within a putative olfactory space, in which each dimension is represented by activity within one of the recorded glomeruli. Similarity between mixture and component representations was globally conserved from AL input to output (Fig. 3A; correlation of

distances between all possible odor pairs from both data sets, $r = 0.66$, $P < 0.001$, df = 103). A PCA revealed three very conspicuous groups of odors, based on their similarity relationships (Fig. 3B, the first two factors represented 66.2% of overall variance). This picture was confirmed by a cluster analysis (Fig. 3C; see PN column). Cluster 1 grouped the two weaker odors (in terms of the number of active glomeruli; see Supplemental Fig. S1A) limonene, linalool, and their binary mixture. Cluster 2 included the strong odor 1-hexanol and all its mixtures with linalool and/or limonene. Cluster 3 grouped the strong odor 2-octanol and all its mixtures and showed a subdivision. One subcluster included all mixtures containing 2-octanol and limonene; the other subcluster contained 2-octanol and all its mixtures with 1-hexanol and linalool. This repartition strongly correlated with that found for the input (Deisig et al. 2006 and Fig. 3C; see compound signal column). Thus although more suppression is evident at the output of the AL, local processing does not modify mixture representation in a drastic way.

Linearity of mixture representations

Similarity relationships among odors found within both the input and the output neural spaces were correlated, but whereas compound signal-based similarity relationships between a mixture and its components could be predicted by an elemental model based on the physiological salience of components (defined as the number of glomeruli activated by each component), a strong and significant departure from the elemental model was observed at the PN level. This is illustrated by the relative Euclidean distances between the representations of each mixture and its components, when calculated in both the glomerular multidimensional input (compound signal, in black) and the output (PN, in white) spaces (Fig. 4A, representative example of the quaternary mixture; Supplemental Fig. S4 shows the same comparison for all mixtures). Bars of equal length correspond to a perfect balance (equidistance) between the components of a mixture (50% for binary, 33% for ternary, and 25% for the quaternary mixture; dotted lines in Fig. 4A and Supplemental Fig. S4). Although compound signal data revealed strongly asymmetrical representations of components in the mixtures (which were explained by different physiological saliences of the components; see following text), component representations in the PN data were more equidistant to their mixture. Components were thus more balanced within mixture representation at the PN level in four of the six binary mixtures, in all ternary and in the quaternary mixture. When analyzing the mean divergence of each component to equidistance in the two data sets (Fig. 4B, 0.29 ± 0.03 for compound signal and 0.17 ± 0.02 for PNs), components were significantly closer to equidistance at the output level than at the input level (paired t -test, df = 26, $P = 0.0012$). As a consequence (Fig. 4C), the elemental principle holding for the input is the stronger a component is (i.e., the more glomeruli it activates), the more similar the mixture is to this component (i.e., the smaller the distance between mixture and component). Indeed, we found a highly linear negative correlation coefficient between these two variables ($r = -0.94$). By contrast, output representation showed a much more scattered trend, with a still negative but lower correlation coefficient ($r = -0.60$). Although both correlations were significant ($P < 0.001$, 26 df),

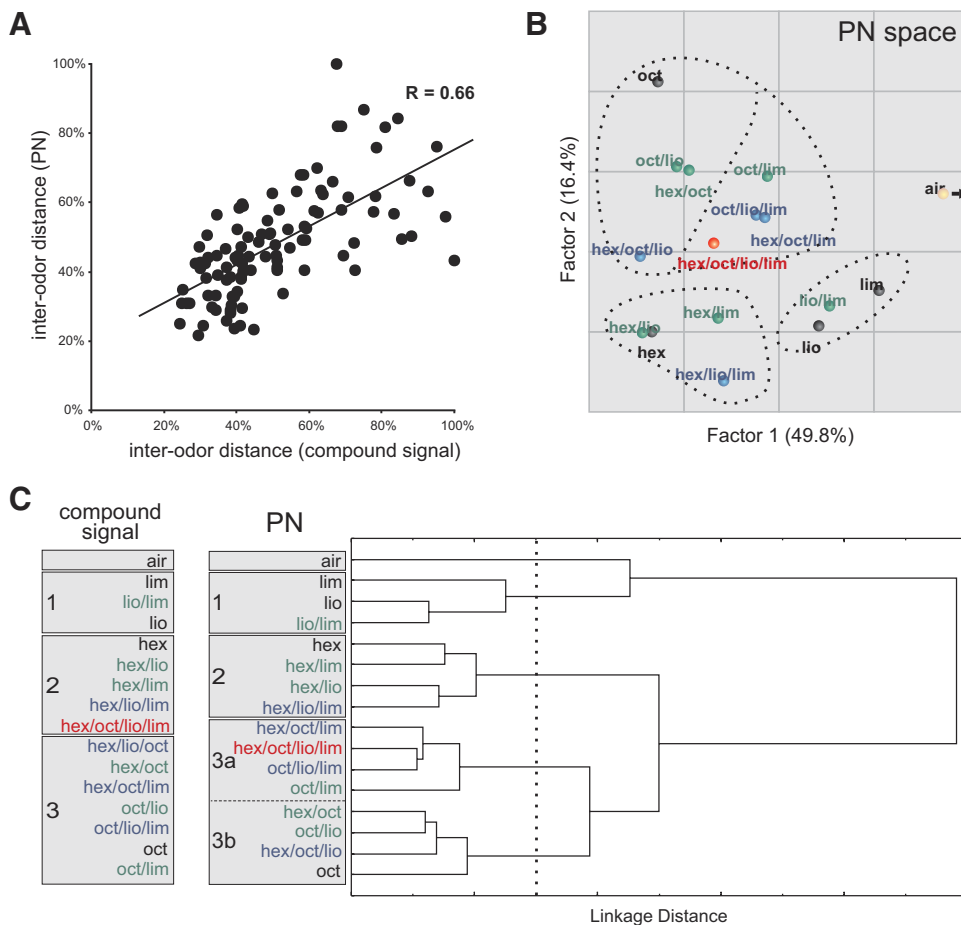


FIG. 3. Coarse odor classification is conserved from AL input to output. *A*: the similarity between 2 odor representations can be measured as the Euclidean distance between odor points in the space of neural activation in which each glomerulus represents a dimension. The graph presents the correlation of Euclidean distances between the 105 possible odor pairs (from the 15 different odors used in our study), at the input (compound signal) and at the output (PNs). The relatively high correlation indicates that global odor similarity relationships are conserved by AL processing ($r = 0.66$, $P < 0.001$, 103 df). *B*: representation of the relative position of odor patterns according to major factors extracted using a principal component analysis (first 2 factors explaining 66.2% of total variance). Three main clusters appear (see dotted lines), as confirmed by a cluster analysis based on Euclidean distances between representations, using Ward's classification method. Three odor clusters emerged (outlined in *B*): 1) limonene and linalool, the 2 weaker odors; 2) hexanol, one of the stronger odors, with all the mixtures of this odor with linalool and/or limonene; and 3) all mixtures containing octanol. This last cluster is further subdivided (see main text). The *right column* and dendrogram correspond to the present PN data. The *left column* shows the classification obtained in the same conditions with the compound signal data (Deisig et al. 2006).

the coefficient for PNs was significantly lower than that obtained for compound signals (homogeneity *t*-test, $P < 0.001$). Thus when compared with the AL input, output mixture representations display a significant departure from the elemental model, which may be attributed to local processing and increased suppression as found before.

Separability between odor representations

What could be the benefit of such fine modifications of mixture representation in the AL? We hypothesized that such reformatting may improve odor separability. To test this idea, we compared Euclidean distances between glomerular activation maps based on normalized input and output data sets. In line with our hypothesis, odor response patterns were significantly more dissimilar, i.e., distances were higher for PNs than those for the compound signal over all possible odor pairs ($n = 105$, Fig. 5*A*, Wilcoxon matched-pair test, $z = 3.06$, $P = 0.002$, $df = 104$). We also found that distances were significantly higher at the PN level for comparisons between any two of the mixtures (Fig. 5*B*, $n = 55$, $z = 2.49$, $P = 0.023$), but not when comparing mixtures to single odors ("elements," Fig. 5*B*, $n = 44$, $z = 1.30$, NS). Comparisons between single odors were also not significant (data not shown, $n = 6$, $z = 1.6$, NS). Thus AL processing increased Euclidean distances between mixture representations. This effect was not due to data normalization because distances between odors and the air control were identical for the compound signal and PN data sets, after

normalization (1.78 ± 0.10 and 1.79 ± 0.09 , respectively, $z = 0.17$, NS). Moreover, this effect was confirmed by using correlation coefficients between response patterns, a measure of pattern similarity that is independent of differences in response intensity in the two data sets. This analysis showed again that output activity patterns were less correlated than input patterns ($n = 105$, Supplemental Fig. S5, $z = 2.37$, $P = 0.017$). This effect appeared for comparisons among mixtures ($z = 5.32$, $P < 0.001$), but was not significant for comparisons between mixtures and single odors ($z = 1.61$, NS). Thus the main effect of AL processing was to decorrelate mixture activity patterns.

Time course of component–mixture relationship

As shown earlier, projection neurons can show polymorphous responses, including phasic, phasic-tonic, and sometimes more complex time courses after stimulus presentation (Sachse and Galizia 2002). We thus asked whether the relationship between mixture and component representations changes with time and thus whether the rules we describe apply throughout the epoch of projection neuron activity. To do this, we computed Euclidean distances between mixture and component representations at each time point, after setting all data to 0 at the first frame (to avoid calculation artifacts before the stimulus). We represented the evolution of the average distance between each mixture type and its components throughout an entire recording (Supplemental Fig. S6). At odor onset, dis-

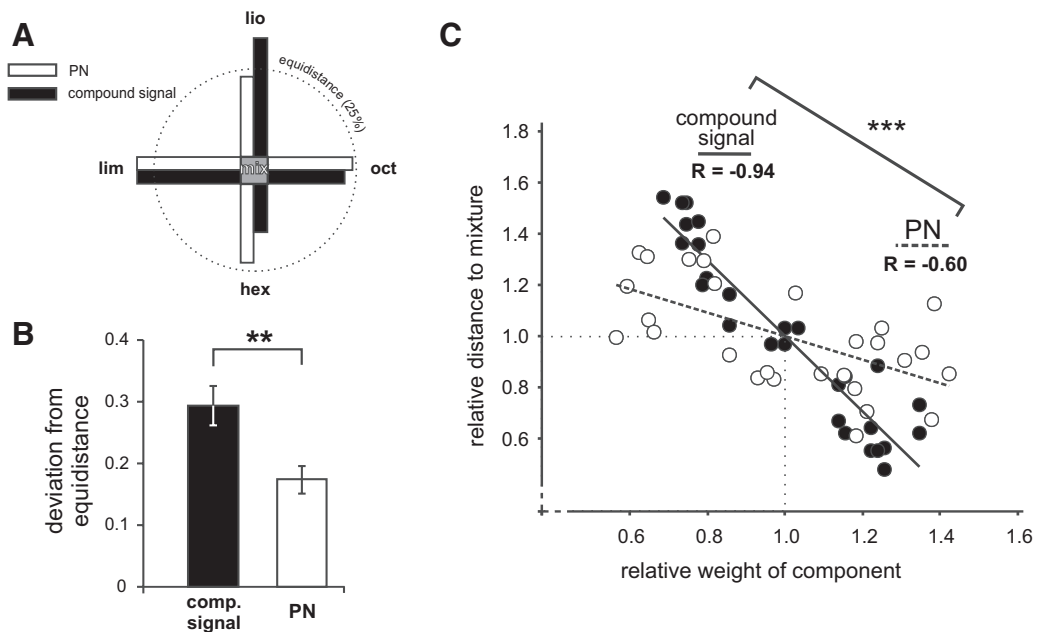


FIG. 4. Antennal lobe processing induces more homogeneous component representation within mixture activity patterns. *A*: relative Euclidean distances between the representations of the quaternary mixture and its components in the glomerular multidimensional input (compound signal, black) and output (PN, white) spaces. In such graphs, the mixture is in the center and the components are on the sides. An equal representation of the components within mixture representation appears as an equidistance of components to the mixture, i.e., as bars of equal length (dotted lines corresponding to 25% for the quaternary mixture). Generally, components appear to be more homogeneously represented (closer to equidistance) at the output level than at the input level (see Supplemental Fig. S4 for more details). *B*: normalized measure of the deviation of each component's representation relative to equidistance (means \pm SE). PN odor representations were significantly closer to equidistance than compound signal representations (paired *t*-test, $P < 0.01$). *C*: evaluation of the elemental model proposed in Deisig et al. (2006) for predicting mixture–component similarity based on simple component information, i.e., the number of glomeruli activated by each odor when presented alone (see text). At the input, the more a component activated the AL when presented alone, the closer it was to the mixture—that is, the more present it was within mixture representation ($R = -0.94$). For PNs, the model does not fit as well ($R = -0.60$), which is mostly due to the homogeneous representation of components in the mixture (see the narrower distribution of PN data on the *y* axis). This suggests a departure from the elemental model at the PN level.

tances between stimuli increased dramatically on stimulus delivery and reached a maximum about 600 ms after stimulus onset, decreasing to near baseline after stimulus offset. The evolution of the distance was the same for all mixture types (binary, ternary, quaternary) and closely followed the evolution of the distance between single odors. When evaluating the correlation between the different curves at signal maximum (2 s during which the distance is at its highest, i.e., 200 to 2,200 ms after stimulus onset; see dotted line in Supplemental Fig. S6), all coefficients were >0.991 . This indicates that the relationships between mixture and component representations follow the same time course throughout a recording.

DISCUSSION

Our study shows that AL processing introduces fine rearrangements in mixture neural representations, so that 1) components are more homogeneously represented within a mixture representation at the PN level than at the input level, 2) mixture representation is less predictable by an elemental model, and 3) odor mixture representations become more separable after AL processing.

Recent works investigated reformatting of odor representation within the AL and compared input and output representations of a range of monomolecular odorants. These studies, performed with different techniques, revealed contrasting processing principles, but led to a similar conclusion. Optical imaging in honeybees illustrated that AL processing sharpens

odor response profiles of PNs, leading to better differentiation between single odorants (Sachse et al. 2002, 2003). By contrast, electrophysiology in fruit flies revealed a broadening of odor response profiles of PNs but, as in bees, this modification led to an improved discrimination between odorants (Bhandawat et al. 2007). Because olfactory mixtures constitute more natural stimuli than monomolecular odors we studied AL-induced modifications in mixture representation. We show that a rather fine rearrangement occurs from AL input to output and that such a rearrangement results in a higher separation power between complex odors. Several studies suggested that mixture representation is rather elemental at the input level (zebra fish: Tabor et al. 2004; bees: Deisig et al. 2006; moths: Carlsson et al. 2007; fruit flies: Silbering et al. 2007), even though within individual ORNs nonlinear responses to mixtures can be observed (Akers and Getz 1993; Cromarty and Derby 1998; Duchamp-Viret et al. 2003). At the output level, studies in the zebrafish (Tabor et al. 2004) and in *Drosophila* (Silbering et al. 2007) showed an increased proportion of cases of nonlinear summation between component signals within individual neurons or glomeruli. Increased suppression phenomena at the PN level in our study fully confirm these accounts (Fig. 2*B*). However, there is an important choice to make when comparing two processing levels, that is 1) focusing on particular units (as in most studies) or 2) describing odor representation in its multidimensional (global) quality (Bhandawat et al. 2007; Broome et al. 2006; this study). Both approaches are certainly helpful; however, the whole odor response pattern seems to

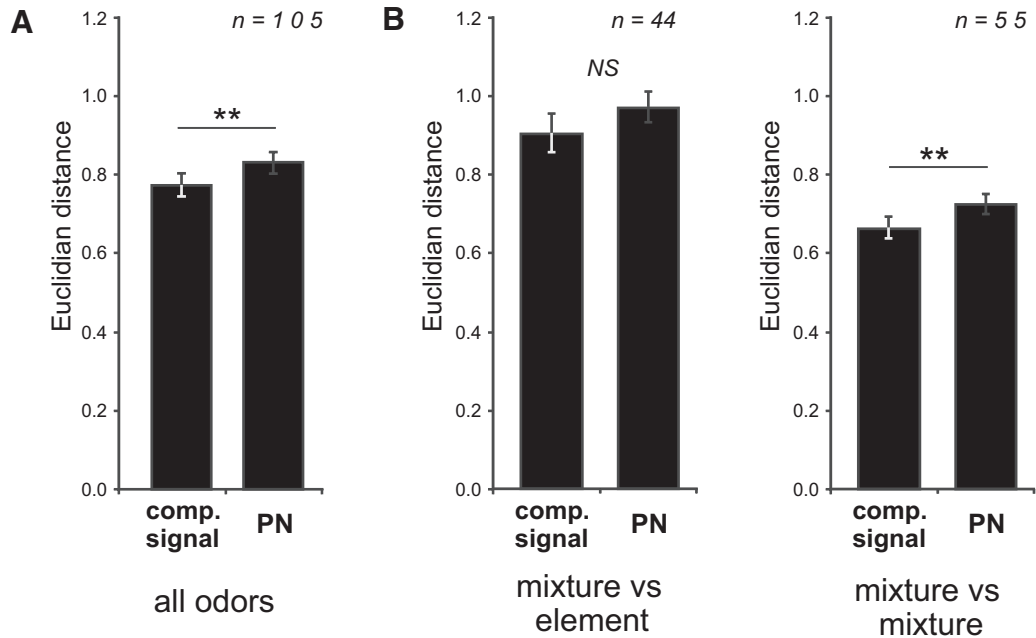


FIG. 5. Antennal lobe processing increases separability between odor mixtures. *A*: Euclidean distances (means \pm SE) were calculated on normalized input (compound signal, black) and output (PN, white) data sets. At the PN level, odors were more separable than at the input level because the mean Euclidean distance between any two odors was significantly higher (Wilcoxon matched-pair test, $P < 0.01$, 104 df). *B*: mean Euclidean distances are shown for comparisons involving (*left*) any mixture and a single odor ("element," $n = 44$ possibilities) and (*right*) any 2 mixtures ($n = 55$ possibilities). Distances were significantly higher at the PN level than at the input level for comparisons involving 2 mixtures (Wilcoxon test, $P < 0.01$). A similar analysis based on correlation coefficients is given in Supplemental Fig. S5. Overall, odor mixture representations are more readily separable at the AL output than at the input.

have more consequence on the animal's behavior than individual units, in that the latter allows predicting olfactory behavior (Guerrieri et al. 2005). Previous studies neither analyzed the multidimensional quality of mixture representation nor did they evaluate the separability of mixture representations at both processing levels. Our study is the first to evaluate these points.

For comparing mixture representation at two processing levels, we used *in vivo* calcium imaging based on two different staining techniques. As with any experimental approach, some cautionary arguments should be made, which relate to 1) the cell populations participating in the signals and 2) the link between calcium signal and neural activity.

CELL TYPES. For the input signal, we bath-applied a permeable calcium sensitive dye, Calcium Green-2 AM, on the brain. With this protocol, all AL cells could be potentially stained (ORNs, PNs, local inhibitory interneurons, glia), but ORNs are by far the most numerous. In addition, the recorded signals are highly stereotyped and never show any spontaneous activity or any inhibitory responses, which are typical for local neurons and PNs (Sachse and Galizia 2002). Therefore the participation of LNs or PNs in the compound signal is thought to be negligible (Galizia and Vetter 2005). A significant part of the signal may come from glial cells surrounding each glomerulus because in the hawkmoth *Manduca sexta*, bath application of Calcium Green was shown to mainly stain periglomerular glial cells in adults and odors trigger activity in these cells (Heil et al. 2007). Even so, it is clearly established that release of acetylcholine (ACh) from ORN axons leads to activation of nicotinic receptors (nAChRs) in these glial cells, which depolarizes the cell membrane and thereby opens voltage-gated calcium channels (VGCCs). In other words, even if glial cells participate in the calcium signal, they do so in a manner

directly correlated to ORN input. We thus interpret the compound signal as mainly representing sensory input. For recording the output representation (present recordings), we used retrograde staining of PNs with fura-2 dextran and the signal was recorded from the glomeruli (i.e., the dendrites of these neurons in the AL). In this case, there is no doubt that only PNs participated in the signal because the dye was injected rather far away from the AL and confocal scans confirmed the specificity of the staining (Sachse et al. 2002; our observation).

CALCIUM SIGNAL AND NEURAL ACTIVITY. The second question relates to the quantitative relationship between the recorded calcium signals and spiking activity of olfactory neurons. Calcium imaging is used as a standard technique for recording neural activity at the network level in many systems (Kwan 2008), since it has been consistently shown that the recorded fluorescence changes are a direct result of calcium influx from action potentials (Kerr et al. 2005) and can be used to reconstruct firing rates efficiently (Yaksi et al. 2006). In our system several arguments indicate a tight link between firing rate and calcium signal. First, recordings of both electrophysiological activity and calcium imaging showed that excitatory (respectively, inhibitory) electrical activity is accompanied by positive (respectively, negative) calcium signals in AL neurons (Galizia and Kimmerle 2004). In addition, calcium imaging of honeybee PNs in primary cell cultures and pharmacological applications performed in our laboratory showed that ACh, which depolarizes the membrane and triggers spiking activity, induces dose-dependent calcium signals predominantly (>80%) through VGCC (V. Raymond-Delpech, A. Augier, T. Jaillard, J. C. Sandoz, unpublished data). Therefore we believe that the calcium signals recorded in our system are closely related to the electrical activity of the neurons.

With these comments in mind, our study shows that AL processing globally conserves the overall structure of the odor space (Fig. 3B) and keeps a similar coarse classification of odor representations (Supplemental Fig. S5). However, AL processing improves fine odor-similarity relationships. A careful evaluation of mixture–component relationships shows that components are more homogeneously represented at the PN level than at the input level (Fig. 4B; see following text). This work also shows for the first time that such interactions bestow improved separability of mixture representations. Both observations suggest that, as in fruit flies (Bhandawat et al. 2007), AL processing produces more uniform distances between odor representations, thereby increasing the global efficiency of the system for odor discrimination (Fig. 5A). In other words, PNs appear to use their multidimensional coding space better than ORNs, both for single odors (Bhandawat et al. 2007) and for odor mixtures (this study). Components were more homogeneously represented within mixture patterns at the PN level (Fig. 4B). This may be a result of the decorrelation of odor representations through AL processing. If AL processing provokes more homogeneously distributed representations in the PN space, it could have the collateral effect of decreasing asymmetries in component–mixture relationships. A direct consequence would be that mixture representation would no longer contain precise information about the relative quantity of its components. If so, PN mixture representation should be more concentration invariant with regard to differences in components' quantity than at the ORN level. Such a property could be important for honeybees, which are “flower constant,” thus limiting their visits to a single plant species as long as it is profitable (Grant 1950). Floral aromas are multicomponent blends that fluctuate in composition according to genotype and flowering stage (Pham-Delègue et al. 1989). Our results indicate that the olfactory system may provide such a component-concentration invariant representation.

Our results fully support a two-tiered model of lateral inhibition in the AL (Sachse and Galizia 2002; Silbering and Galizia 2007), with one tier representing homogeneous inhibition, playing the role of a gain control and a second tier representing heterogeneous, asymmetrical inhibition between glomeruli. We observed the first tier at the input level because inhibition reduced overall signal strength, thereby avoiding saturating the system, but kept elemental information within mixture representation (Deisig et al. 2006). PN results point to the second tier, with an inhibitory system provoking more interactions between components within mixture signals and modifying fine odor-similarity relationships. Such a system could explain the observed departure from elemental mixture representation. What could be the neural basis of such a model? The honeybee AL contains two main anatomical types of local inhibitory interneurons, possibly representing the two tiers: roughly 13% of the 4,000 local interneurons diffuse homogeneously in the AL (homo-LNs), whereas the rest show a high branching density in one particular glomerulus (hetero-LNs: Flanagan and Mercer 1989; Fonta et al. 1993). Homo-LNs would be involved in gain control (first tier) and are thought to represent a picrotoxin-sensitive network, based on GABAergic neurotransmission (Sachse and Galizia 2002). On the other hand, hetero-LNs would accomplish focused lateral inhibition between physiologically neighbor glomeruli (second tier) and would constitute a picrotoxin-insensitive network

(Sachse and Galizia 2002). The neurotransmitter for this second tier is still unknown. Recently, a histaminergic inhibitory system has been proposed (Sachse et al. 2006), but it likely belongs to the first tier because histamine-immunoreactive interneurons are few (~35 LNs; Bornhauser and Meyer 1997) and histamine application during calcium imaging already provokes a strong reduction of odor-evoked signals at the input level (Sachse et al. 2006). Other candidates could be glutamate (Barbara et al. 2005; El Hassani et al. 2008), but also γ -aminobutyric acid through possible picrotoxin-insensitive heteromeric chloride channels (Dupuis et al. 2010). In contrast to *Drosophila*, up to now, no excitatory interneurons have been found in the bee.

The honeybee olfactory system is mainly organized along two parallel pathways, with two main types of uniglomerular PNs taking information from different subsets of AL glomeruli (Abel et al. 2001; Kirschner et al. 2006; Müller et al. 2002). Comparing the rules described here for lateral-ACT neurons with those of the second population (median-ACT) could be especially promising: l-ACT neurons could provide the brain with component-composition invariant information, whereas m-ACT neurons would keep track of relative component quantities. A necessary step should thus be the study of the subsequent reformatting of mixture representations in higher-order brain centers. The strong sparsening of odor representation from PNs to Kenyon cells, the intrinsic mushroom body neurons (Perez-Orive et al. 2002; Szyszka et al. 2005), and their coincidence detection properties (Jortner et al. 2007) could be the basis for mixture-specific units, as in the mouse olfactory cortex. There, about 30% of all recorded neurons were mixture specific, responding to binary mixtures, but not to either of their components (Zou and Buck 2006). Whether equivalent units exist in the mushroom bodies remains to be tested.

ACKNOWLEDGMENTS

We thank H. Lachnit for helpful comments.

Present addresses: N. Deisig, Insect Physiology (UMR 1272), INRA, Versailles, France; and J. C. Sandoz, Evolution, Genome and Speciation (UPR 9034), CNRS, Gif-sur-Yvette, France.

GRANTS

This work was supported by funds from the Action Concertée Incitative Biologie Cellulaire Moléculaire et Structurale and Neurosciences Intégratives et Computationnelles from the French Research Ministry to M. Giurfa. M. Giurfa and J. C. Sandoz were supported by the University Paul-Sabatier and the French Research Council of Centre National de la Recherche Scientifique (CNRS). N. Deisig was supported by the Fyssen Foundation and the CNRS.

DISCLOSURES

No conflicts of interest are declared by the authors.

REFERENCES

- Akers RP, Getz WM. Response of olfactory receptor neurons in honeybees to odorants and their binary mixtures. *J Comp Physiol A Sens Neural Behav Physiol* 173: 169–185, 1993.
- Barbara GS, Zube C, Rybak J, Gauthier M, Grünwald B. Acetylcholine, GABA and glutamate induce ionic currents in cultured antennal lobe neurons of the honeybee, *Apis mellifera*. *J Comp Physiol A Sens Neural Behav Physiol* 191: 823–836, 2005.
- Bhandawat V, Olsen SR, Gouwens NW, Schlieff ML, Wilson RI. Sensory processing in the *Drosophila* antennal lobe increases reliability and separability of ensemble odor representations. *Nat Neurosci* 10: 1474–1482, 2007.

- Bornhauser BC, Meyer EP.** Histamine-like immunoreactivity in the visual system and brain of an orthopteran and a hymenopteran insect. *Cell Tissue Res* 287: 211–221, 1997.
- Broome BM, Jayaraman V, Laurent G.** Encoding and decoding of overlapping odor sequences. *Neuron* 51: 467–482, 2006.
- Carlsson MA, Chong KY, Daniels W, Hansson BS, Pearce TC.** Component information is preserved in glomerular responses to binary odor mixtures in the moth *Spodoptera littoralis*. *Chem Senses* 32: 433–443, 2007.
- Cromarty SI, Derby CD.** Inhibitory receptor binding events among the components of complex mixtures contribute to mixture suppression in responses of olfactory receptor neurons of spiny lobsters. *J Comp Physiol A Sens Neural Behav Physiol* 183: 699–707, 1998.
- Deisig N, Giurfa M, Lachnit H, Sandoz JC.** Neural representation of olfactory mixtures in the honeybee antennal lobe. *Eur J Neurosci* 24: 1161–1174, 2006.
- Duchamp-Viret P, Duchamp A, Chaput MA.** Single olfactory sensory neurons simultaneously integrate the components of an odour mixture. *Eur J Neurosci* 18: 2690–2696, 2003.
- Dupuis JP, Bazelot M, Barbara GS, Paute S, Gauthier M, Raymond-Delpech V.** Homomeric RDL and heteromeric RDL/LCCH3 GABA receptors in the honeybee antennal lobes: two candidates for inhibitory transmission in olfactory processing. *J Neurophysiol* 103: 458–468, 2010.
- El Hassani AK, Giurfa M, Gauthier M, Armengaud C.** Inhibitory neurotransmission and olfactory memory in honeybees. *Neurobiol Learn Mem* 90: 589–595, 2008.
- Flanagan D, Mercer AR.** An atlas and 3-D reconstruction of the antennal lobes in the worker honey bee, *Apis mellifera* L. (Hymenoptera: Apidae). *Int J Insect Morphol Embryol* 18: 145–159, 1989.
- Fonta C, Sun XJ, Masson C.** Morphology and spatial distribution of bee antennal lobe interneurons responsive to odours. *Chem Senses* 18: 101–119, 1993.
- Galizia CG, Kimmerle B.** Physiological and morphological characterization of honeybee olfactory neurons combining electrophysiology, calcium imaging and confocal microscopy. *J Comp Physiol A Sens Neural Behav Physiol* 190: 21–38, 2004.
- Galizia CG, McIlwrath SL, Menzel R.** A digital three-dimensional atlas of the honeybee antennal lobe based on optical sections acquired using confocal microscopy. *Cell Tissue Res* 295: 383–394, 1999.
- Galizia CG, Nägler K, Hölldobler B, Menzel R.** Odour coding is bilaterally symmetrical in the antennal lobe of honeybees (*Apis mellifera*). *Eur J Neurosci* 10: 2964–2974, 1998.
- Galizia CG, Vetter R.** Optical methods for analyzing odor-evoked activity in the insect brain. In: *Advances in Insect Sensory Neuroscience*, edited by Christensen TA. Boca Raton, FL: CRC Press, 2005, p. 349–392.
- Grant V.** The flower constancy of bees. *Bot Rev* 3: 82–97, 1950.
- Guerrieri F, Schubert M, Sandoz JC, Giurfa M.** Perceptual and neural olfactory similarity in honeybees. *PLoS Biol* 3: e60, 2005.
- Heil JE, Oland LA, Lohr C.** Acetylcholine-mediated axon-glia signaling in the developing insect olfactory system. *Eur J Neurosci* 26: 1227–1241, 2007.
- Jortner RA, Farivar SS, Laurent G.** A simple connectivity scheme for sparse coding in an olfactory system. *J Neurosci* 27: 1659–1669, 2007.
- Kerr JND, Greenberg D, Helmchen F.** Imaging input and output of neocortical networks in vivo. *Proc Natl Acad Sci USA* 102: 14063–14068, 2005.
- Kwan AC.** What can population calcium imaging tell us about neural circuits? *J Neurophysiol* 100: 2977–2980, 2008.
- Laurent G.** Olfactory network dynamics and the coding of multidimensional signals. *Nat Rev Neurosci* 3: 884–895, 2002.
- Mombaerts P, Wang F, Dulac C, Chao SK, Nemes A, Mendelsohn M, Edmondson J, Axel R.** Visualizing an olfactory sensory map. *Cell* 87: 675–686, 1996.
- Müller D, Abel R, Brandt R, Zockler M, Menzel R.** Differential parallel processing of olfactory information in the honeybee, *Apis mellifera* L. *J Comp Physiol A Sens Neural Behav Physiol* 188: 359–370, 2002.
- Ng M, Roorda RD, Lima SQ, Zemelman BV, Morcillo P, Miesenböck G.** Transmission of olfactory information between three populations of neurons in the antennal lobe of the fly. *Neuron* 36: 463–474, 2002.
- Peele P, Ditzén M, Menzel R, Galizia CG.** Appetitive odor learning does not change olfactory coding in a subpopulation of honeybee antennal lobe neurons. *J Comp Physiol A Sens Neural Behav Physiol* 192: 1083–1103, 2006.
- Perez-Orive J, Mazor O, Turner GC, Cassenaer S, Wilson RI, Laurent G.** Oscillations and sparsening of odor representations in the mushroom body. *Science* 297: 359–365, 2002.
- Pham-Delegue MH, Etiévant P, Guichard E, Masson C.** Sunflower volatiles involved in honeybee discrimination among genotypes and flowering stages. *J Chem Ecol* 15: 329–343, 1989.
- Root CM, Semmelhack JL, Wong AM, Flores J, Wang JW.** Propagation of olfactory information in *Drosophila*. *Proc Natl Acad Sci USA* 104: 11826–11831, 2007.
- Sachse S, Galizia CG.** The role of inhibition for temporal and spatial odor representation in olfactory output neurons: a calcium imaging study. *J Neurophysiol* 87: 1106–1117, 2002.
- Sachse S, Galizia CG.** The coding of odour-intensity in the honeybee antennal lobe: local computation optimizes odour representation. *Eur J Neurosci* 18: 2119–2132, 2003.
- Sachse S, Peele P, Silbering AF, Guhmann M, Galizia CG.** Role of histamine as a putative inhibitory transmitter in the honeybee antennal lobe (Abstract). *Front Zool* 3: 22, 2006.
- Sachse S, Rappert A, Galizia CG.** The spatial representation of chemical structures in the antennal lobe of honeybees: steps towards the olfactory code. *Eur J Neurosci* 11: 3970–3982, 1999.
- Sandoz JC.** Odour-evoked responses to queen pheromone components and to plant odours using optical imaging in the antennal lobe of the honey bee drone *Apis mellifera* L. *J Exp Biol* 209: 3587–3598, 2006.
- Silbering AF, Galizia CG.** Processing of odor mixtures in the *Drosophila* antennal lobe reveals both global inhibition and glomerulus-specific interactions. *J Neurosci* 27: 11966–11977, 2007.
- Szyszkka P, Ditzén M, Galkin A, Galizia CG, Menzel R.** Sparsening and temporal sharpening of olfactory representations in the honeybee mushroom bodies. *J Neurophysiol* 94: 3303–3313, 2005.
- Tabor R, Yaksi E, Weislogel JM, Friedrich RW.** Processing of odor mixtures in the zebrafish olfactory bulb. *J Neurosci* 24: 6611–6620, 2004.
- Vosshall LB, Wong AM, Axel R.** An olfactory sensory map in the fly brain. *Cell* 102: 147–159, 2000.
- Wachowiak M, Shipley MT.** Coding and synaptic processing of sensory information in the glomerular layer of the olfactory bulb. *Semin Cell Dev Biol* 17: 411–423, 2006.
- Wang JW, Wong AM, Flores J, Vosshall LB, Axel R.** Two-photon calcium imaging reveals an odor-evoked map of activity in the fly brain. *Cell* 112: 271–282, 2003.
- Wilson RI, Turner GC, Laurent G.** Transformation of olfactory representations in the *Drosophila* antennal lobe. *Science* 303: 366–370, 2004.
- Yaksi E, Friedrich RW.** Reconstruction of firing rate changes across neuronal populations by temporally deconvolved Ca²⁺ imaging. *Nature Methods* 3: 377–383, 2006.
- Zou Z, Buck LB.** Combinatorial effects of odorant mixes in olfactory cortex. *Science* 311: 1477–1481, 2006.